0026-895X/09/7602-342–355$20.00
MOLECULAR PHARMACOLOGY
Copyright © 2009 The American Society for Pharmacology and Experimental Therapeutics
Mol Pharmacol 76:342–355, 2009

Vol. 76, No. 2
56523/3499960
Printed in U.S.A.

Sorafenib and Vorinostat Kill Colon Cancer Cells by CD95-Dependent and -Independent Mechanisms

Teneille Walker, Clint Mitchell, Margaret A. Park, Adly Yacoub, Martin Graf, Mohamed Rahmani, Peter J. Houghton, Christina Voelkel-Johnson, Steven Grant, and Paul Dent

Departments of Biochemistry (P.D., T.W., C.M., M.A.P., S.G.), Medicine (S.G., M.R.), Radiation Oncology (A.Y.), and Neurosurgery (M.G.) and Institute for Molecular Medicine (P.D., S.G.), Virginia Commonwealth University, Richmond, Virginia; Department of Microbiology and Immunology, Medical University of South Carolina, Charleston, South Carolina (C.V.J.); and Department of Molecular Pharmacology, St. Jude Children's Research Hospital, Memphis, Tennessee (P.J.H.)

Received March 25, 2009; accepted May 27, 2009

ABSTRACT

We examined the interaction between the multikinase inhibitor sorafenib and histone deacetylase inhibitors. Sorafenib and vorinostat synergized (sorafenib + vorinostat) to kill HCT116 and SW480 cells. In SW480 cells, sorafenib + vorinostat increased CD95 plasma membrane levels and promoted death-inducing signal complex (DISC) formation, and drug toxicity was blocked by knockdown of CD95 or overexpression of cellular FLICE-like inhibitory protein (c-FLIP-s). In SW620 cells that are patient-matched to SW480 cells, sorafenib + vorinostat toxicity was significantly lower, which correlated with a lack of CD95 activation and lower expression of ceramide synthase 6 (LASS6). Overexpression of LASS6 in SW620 cells enhanced drug-induced CD95 activation and enhanced tumor cell killing, whereas knockdown of LASS6 in SW480 cells suppressed CD95 activation. Knocking down LASS6 expression also suppressed CD95 activation in hepatoma, pancreatic, and ovarian cancer cells. In HCT116 cells, sorafenib + vorinostat treatment caused DISC formation without reducing c-FLIP-s expression and did not increase CD95 plasma membrane levels; sorafenib + vorinostat exposure killed HCT116 cells via an intrinsic pathway/caspase 9-dependent mechanism. In HCT116 cells, knockdown of CD95 *enhanced* sorafenib + vorinostat lethality, which correlated with less drug-induced CD95-dependent autophagy. Sorafenib + vorinostat treatment activated the c-Jun NH_2-terminal kinase pathway, which was causal in promoting dissociation of Beclin1 from BCL-2, and in promoting autophagy. Knockdown of Beclin1 expression blocked autophagy and enhanced drug toxicity. Our data demonstrate that treatment of colon cancer cells with sorafenib + vorinostat activates CD95 via de novo ceramide synthesis that promotes viability via autophagy or degrades survival via either the extrinsic or intrinsic pathways.

In the United States, colon cancer is diagnosed in ~150,000 patients each year, and there are ~50,000 deaths from the disease, which has a 5-year survival rate of ~60% (Parkin et al., 2005; Hegde et al., 2008). However, for patients with nonlocalized tumor at diagnosis, the 5-year survival rate is ~10%.

The Raf-MEK1/2-ERK1/2 pathway is frequently dysregulated in neoplastic transformation (Dent et al., 2003; Dent, 2005; Valerie et al., 2007). The MEK1/2-ERK1/2 module comprises, along with c-Jun NH_2-terminal kinase (JNK1/2) and p38 MAPK, members of the MAPK superfamily. These kinases are involved in responses to diverse mitogens and environmental stresses and have also been implicated in cell survival processes. Activation of the ERK1/2 pathway is often associated with cell survival, whereas JNK1/2 and p38 MAPK pathway signaling often causes apoptosis. Although

This work was funded by the National Institutes of Health National Institute of Diabetes and Digestive and Kidney Diseases [Grant R01-DK52825]; the National Institutes of Health National Cancer Institute [Grants P01-CA104177, R01-CA108520, R01-CA63753, R01-CA77141, R01-CA93738]; by The Jimmy V Foundation; and by The Goodwin Foundation for Cancer Research (to Massey Cancer Center). P.D. is the holder of the Universal Inc. Professorship in Signal Transduction Research.

Article, publication date, and citation information can be found at http://molpharm.aspetjournals.org.

doi:10.1124/mol.109.056523.

ABBREVIATIONS: MEK, mitogen activated extracellular regulated kinase; ERK, extracellular regulated kinase; JNK, c-Jun NH_2-terminal kinase; MAPK, mitogen activated protein kinase; c-FLIP, cellular FLICE-like inhibitory protein; PERK, protein kinase-like endoplasmic reticulum kinase; ER, endoplasmic reticulum; PI3K, phosphatidyl inositol 3 kinase; MCL-1, myeloid cell leukemia sequence 1 (BCL2-related); HDACI, histone deacetylase inhibitor; CMV, cytomegalovirus; DMSO, dimethyl sulfoxide; GX15-070, obatoclax; dn, dominant negative; CI, combination index; DISC, death-inducing signal complex; ASMase, acidic sphingomyelinase; LASS6, ceramide synthase 6; eIF2α, eukaryotic initiation factor 2α; BCL-2, B-cell lymphoma 2; FITC, fluorescein isothiocyanate; PAGE, polyacrylamide gel electrophoresis; siSCR, scrambled siRNA.

the mechanisms by which ERK1/2 activation promote survival are not fully characterized, a number of antiapoptotic effector proteins have been identified, including increased expression of antiapoptotic proteins such as c-FLIP (Allan et al., 2003; Ley et al., 2003; Mori et al., 2003; Qiao et al., 2003; Grant and Dent, 2004; Wang et al., 2007). In view of the importance of the RAF-MEK1/2-ERK1/2 pathway in neoplastic cell survival, inhibitors have been developed that have entered clinical trials, including sorafenib (Bay 43-9006; Nexavar; a Raf kinase inhibitor) and a MEK1/2 inhibitor (Davies et al., 2007; Li et al., 2007).

Sorafenib is a multikinase inhibitor that was originally developed as an inhibitor of Raf-1 but was subsequently shown to inhibit multiple other kinases, including class III tyrosine kinase receptors such as platelet-derived growth factor, vascular endothelial growth factor receptors 1 and 2, c-Kit, and FLT3 (Flaherty, 2007). Antitumor effects of sorafenib in renal cell carcinoma and in hepatoma have been ascribed to antiangiogenic actions of this agent through inhibition of the growth factor receptors (Gollob, 2005; Strumberg, 2005; Rini, 2006). Several groups, including ours, have shown in vitro that sorafenib kills human leukemia cells at concentrations below the maximum achievable dose (C_{max}) of 15 to 20 μM, through a mechanism involving down-regulation of the antiapoptotic BCL-2 family member MCL-1 (Rahmani et al., 2005, 2007a). In these studies, sorafenib-mediated MCL-1 down-regulation occurred through a translational rather than a transcriptional or post-translational process that was mediated by endoplasmic reticulum (ER) stress signaling (Dasmahapatra et al., 2007; Rahmani et al., 2007b). This suggests that the previously observed antitumor effects of sorafenib are mediated by a combination of inhibition of *Raf* family kinases and the ERK1/2 pathway, receptor tyrosine kinases that signal angiogenesis, and the induction of ER stress signaling.

Histone deacetylase inhibitors (HDACI) represent a class of agents that act by blocking histone deacetylation, thereby modifying chromatin structure and gene transcription. Histone deacetylases, along with histone acetyltransferases, reciprocally regulate the acetylation status of the positively charged NH_2-terminal histone tails of nucleosomes. HDACIs promote histone acetylation and neutralization of positively charged lysine residues on histone tails, allowing chromatin to assume a more open conformation, which favors transcription (Gregory et al., 2001). However, HDACIs also induce acetylation of other nonhistone targets, actions that may have pleiotropic biological consequences, including inhibition of 90-kDa heat shock protein function, induction of oxidative injury, and up-regulation of death receptor expression (Kwon et al., 2002; Marks et al., 2003; Bali et al., 2005). With respect to combinatorial drug studies with a multikinase inhibitor such as sorafenib, HDACIs are of interest in that they have potential to down-regulate multiple oncogenic kinases by interfering with 90-kDa heat shock protein function, leading to proteasomal degradation of these proteins. Vorinostat (suberoylanilide hydroxamic acid; Zolinza) is a hydroxamic acid HDACI that has shown preliminary preclinical evidence of activity in hepatoma and other malignancies with a C_{max} of ~9 μM (Pang and Poon, 2007; Venturelli et al., 2007; Wise et al., 2007).

We recently reported that sorafenib and vorinostat interact to kill in renal, hepatocellular and pancreatic carcinoma cells via activation of the CD95 extrinsic apoptotic pathway, concomitant with drug-induced reduced expression of c-FLIP-s via RNA-activated protein kinase-like endoplasmic reticulum kinase (PERK) signaling to eIF2α (Park et al., 2008a; Zhang et al., 2008). Subsequent work mechanistically advanced our understanding to reveal that sorafenib and vorinostat interact by activating acidic sphingomyelinase and the de novo ceramide pathway to promote CD95 activation, which regulates both apoptosis and autophagy. The present studies determined whether the same killing mechanisms apply after sorafenib and vorinostat treatment in colon cancer cells.

Materials and Methods

Materials

The vorinostat, sorafenib, and obatoclax used in this manuscript were generously provided by Merck and Co., Inc. (Darmstadt, Germany), Bayer Corp., Pharmaceutical Div. (West Haven, CT), and Gemin X Pharmaceuticals (Malvern, PA), respectively, and by the National Cancer Institute (Bethesda, MD). Primary antibodies were purchased from Cell Signaling Technologies (Ipswich, MA). HCT116, SW480, SW620, DLD1, PANC1, HEPG2, OVCAR, and SKOVIII carcinoma cells were purchased from the American Type Culture Collection (Manassas, VA). SW620 cells expressing LASS6 were provided by author C.V.-J. Rh30 and Rh41 rhabdomyosarcoma cells were provided by author P.J.H. HCT116 parental cells that express K-RAS Asp13 and were transfected with CMV empty vector; HCT116 cells deleted for the single allele of K-RAS Asp13; HCT116 cells deleted for K-RAS Asp13 stably expressing H-RAS Val12 and also transfected with effector mutants of H-RAS Val12 were as described in Ihle et al. (2009). Commercially available validated short hairpin RNA molecules to knockdown RNA/protein levels were from QIAGEN (Valencia, CA): CD95 (Hs_FAS_7 HP validated siRNA; Hs_FAS_10 HP siRNA); ATG5 (Hs_APG5L_6 HP validated siRNA); Beclin 1 (Hs_BECN1_1 HP siRNA, Hs_BECN1_3 HP siRNA). We used, for confirmatory purposes, the short hairpin RNA construct targeting *ATG5* (pLVTHM/Atg5), which was a generous gift from Dr. S. Yousefi, Department of Pharmacology, University of Bern, Bern Switzerland. The plasmids to express green fluorescent protein (GFP)-tagged human LC3; wild-type and dominant negative PERK (Myc-tagged PERKΔC); were kindly provided by Dr. S. Spiegel (Virginia Commonwealth University, Richmond, VA) and Dr. J. A. Diehl (University of Pennsylvania, Philadelphia, PA). Reagents and performance of experimental procedures were described previously (Qiao et al., 2001; Mitchell et al., 2007; Rahmani et al., 2007a,b; Park et al., 2008a,b,c; Yacoub et al., 2008; Zhang et al., 2008).

Methods

Culture and In Vitro Exposure of Cells to Drugs. All established cell lines were cultured at 37°C [5% (v/v) CO_2] in vitro using RPMI 1640 medium supplemented with 5% (v/v) fetal calf serum and 10% (v/v) nonessential amino acids. For short-term cell killing assays and immunoblotting studies, cells were plated at a density of 3×10^3 cells/cm^2 (~2×10^5 cells/well of a 12-well plate) and 48 h after plating were treated with various drugs, as indicated. In vitro vorinostat and sorafenib treatments were from 100 mM stock solutions of each drug, and the maximal concentration of vehicle (DMSO) in media was 0.02% (v/v). Cells were not cultured in reduced serum

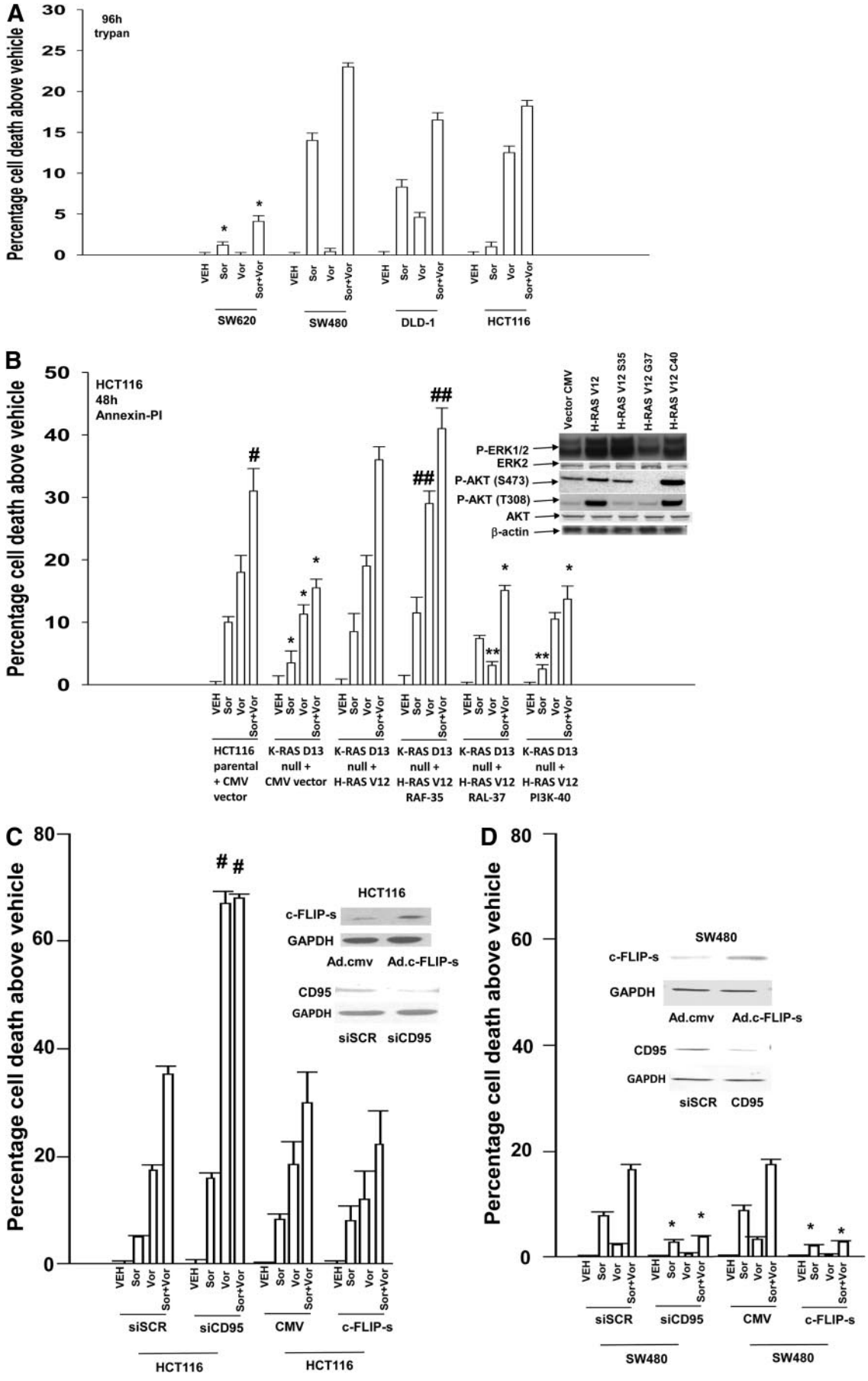

Fig. 1.

media during any study reported in this article. HCT116 (parental and transfected variants thereof), HEPG2, OVCAR, Rh30, Rh41, and SKOVIII cells were treated in all studies with 3 μM sorafenib unless otherwise indicated. PANC1, SW620, SW480, and DLD1 cells were treated in all studies with 6 μM sorafenib unless otherwise indicated. Cells were treated with 500 nM vorinostat and 1.0 mM sodium valproate unless otherwise indicated. Cells were treated with 100 nM obatoclax (GX15-070) unless otherwise indicated.

In Vitro Cell Treatments, Microscopy, SDS-PAGE, and Western Blot Analysis. For in vitro analyses of short-term cell death effects, cells were treated with vehicle, vorinostat, or the combination of sodium valproate and sorafenib (sodium valproate + sorafenib) for the times indicated in the figure legends. For apoptosis assays where indicated, cells were pretreated with vehicle (DMSO) and therapeutic drugs; cells were isolated at the indicated times and subjected to trypan blue cell viability assay by counting in a light microscope. Alternatively, the Annexin V/propidium iodide assay was carried out to determine cell viability according to the manufacturer's instructions (BD Pharmingen, San Diego, CA) using a FACScan flow cytometer (BD Biosciences, San Jose, CA).

For SDS-PAGE and immunoblotting, cells after the time of treatment indicated in the figure legends, were lysed in whole-cell lysis buffer (0.5 M Tris-HCl, pH 6.8, 2% SDS, 10% glycerol, 1% β-mercaptoethanol, and 0.02% bromphenol blue), and the samples were boiled for 30 min. The boiled samples were loaded onto 10 to 14% SDS-PAGE, and electrophoresis was run overnight. Proteins were electrophoretically transferred onto 0.22-μm nitrocellulose, and immunoblotted with various primary antibodies against different proteins. All immunoblots were visualized by an Odyssey Infra Red Imaging system (LI-COR Biosciences, Lincoln, NE). For presentation, immunoblots were digitally processed at 600 dots per inch using PhotoShop CS2 (Adobe Systems, Mountain View, CA) and their color was removed; and figures were generated with the use of PowerPoint (Microsoft Corp., Redmond, WA).

Infection of Cells with Recombinant Adenoviruses. Cells were plated at 3×10^3cells/cm^2 in each well of a 12-well, 6-well, or 60-mm plate. After plating (24 h), cells were infected (hepatoma and pancreatic carcinoma at a multiplicity of infection of 50) with a control empty vector virus (CMV) and adenoviruses to express MEK1 EE, constitutively active AKT, dnMEK1, dnAKT, CRM A, c-FLIP-s, BCL-XL, or XIAP (Vector Biolabs, Philadelphia, PA). After infection (24 h), cells were treated with the concentrations of vorinostat or sodium valproate + sorafenib and/or other drugs indicated under *Methods*, and cell survival or changes in expression/phosphorylation were determined 0 to 96 h after drug treatment.

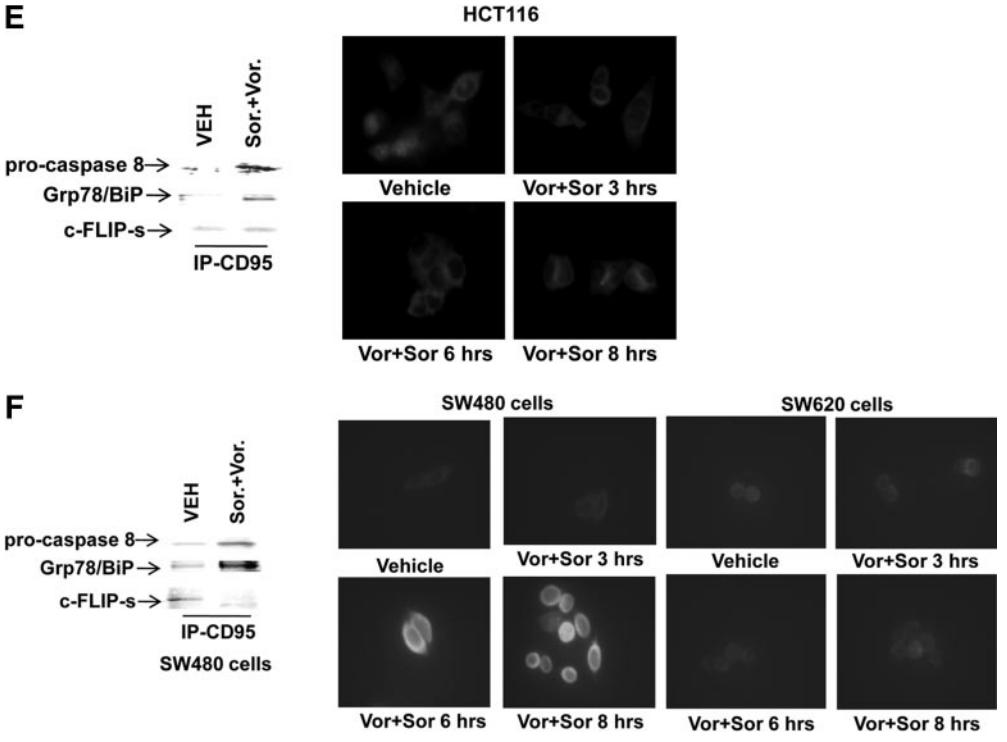

Fig. 1. Sorafenib and vorinostat interact to kill multiple human colon cancer cell lines. A, SW620, SW480, DLD-1, and HCT116 cells were treated with vehicle, sorafenib, vorinostat, or sorafenib + vorinostat. Ninety-six hours after exposure, cells were isolated, and viability was determined via trypan blue exclusion assay (± S.E.M., $n = 3$ independent studies) $* p < 0.05$ bottom than corresponding value in SW480 cells. B, parental and transfected variants of HCT116 cells were treated with vehicle, sorafenib, vorinostat, or sorafenib + vorinostat. Forty-eight hours after exposure, cells were isolated and stained with Annexin V-propidium iodide, and cell viability was determined by flow cytometry (± S.E.M., $n = 3$) #, $p < 0.05$ greater than sorafenib or vorinostat treatment alone; ##, $p < 0.05$ greater than corresponding value in parental + CMV vector cells; $*$, $p < 0.05$ less than corresponding value in parental + CMV vector cells; $**$, $p < 0.05$ less than corresponding value in K-RAS Asp13 null + H-RAS Val12 cells. Inset, immunoblotting of untreated cells for the basal levels of phosphorylation of ERK1/2 and AKT (Ser473; Thr308) in the HCT116 isolates. C and D, HCT116 or SW480 cells were, as indicated, either infected with recombinant adenoviruses or transfected with siRNA molecules to knock down CD95. Twenty-four hours after infection or transfection, cells were treated with vehicle, sorafenib, vorinostat, or both drugs together. Forty-eight hours after exposure, cells were isolated and stained with Annexin V-propidium iodide, and cell viability was determined by flow cytometry (± S.E.M., $n = 3$); $*$, $p < 0.05$ less than corresponding value in CMV vector or siSCR control cells. Immunoblots show CD95 knockdown and c-FLIP-s protein expression under the indicated conditions. E and F, HCT116, SW480, and SW620 cells were plated in eight-well glass chamber slides and were treated with vehicle or sorafenib + vorinostat. Cells were fixed and not permeabilized 0 to 8 h after drug exposure. Fixed cells were immunostained for plasma membrane-associated CD95 and visualized using a FITC-conjugated secondary antibody. Images are representatives from two separate studies. In parallel, HCT116 and SW480 cells were treated with vehicle or with sorafenib + vorinostat. Six hours after treatment, cells were lysed and CD95-immunoprecipitated. Immunoprecipitates were subjected to SDS-PAGE and immunoblotting. A representative CD95 immunoprecipitate is shown ($n = 3$).

Transfection of Cells with siRNA or with Plasmids. Transfection protocols were identical to those performed as described previously (Park et al., 2008a; Zhang et al., 2008), with siRNA transfection at 20 nM.

CD95 Cell Surface Density Measurement. Five random cells were selected from each treatment condition. The density of CD95 staining was measured at 50 points per cell under a fluorescent microscope using Axiocam/Axiovision imaging software (Carl Zeiss, Thornburg, NY).

Data Analysis. Comparison of the effects of various treatments was performed using analysis of variance and the Student's *t* test. Differences with a p value of < 0.05 were considered statistically significant. Experiments shown are the means of multiple individual points (± S.E.M.). Median dose-effect isobologram analyses are a quantitative assessment to determine whether drug interactions were additive or synergistic. Synergy calculations were performed according to the method of T.-C. Chou and P. Talalay using the Calcusyn program for Windows (BIOSOFT, Cambridge, UK). A combination index (CI) value of less than 1.00 indicates synergy of interaction between the drugs, a value of 1.00 indicates additivity, and a value of >1.00 equates to antagonism of action between the agents.

Results

In short-term cell viability assays, sorafenib and vorinostat interacted in an additive to greater-than-additive manner to kill SW480, DLD-1, and HCT116 colon cancer cells (Fig. 1A). It is noteworthy that whereas sorafenib and vorinostat interacted in a greater-than-additive manner to kill SW480 cells, patient-matched SW620 cells were resistant to drug-induced lethality. HCT116 cells and variants of HCT116 cells that are genetically deleted for K-RAS Asp13 and transfected with empty vector (CMV) and H-RAS Val12 or effector mutants of H-RAS Val12 that activate specific downstream pathways were next treated with sorafenib and vorinostat. The H-RAS Val12 effector mutants selectively activate RAF (H-RAS Val12–Ser35), ral guanine nucleotide dissociation stimulator (H-RAS Val12–Gly37), and PI3K (H-RAS Val12–Cys40), respectively. Sorafenib and vorinostat toxicity was reduced in tumor cells lacking mutant active K-RAS Asp13 expression, was restored in cells expressing H-RAS Val12, and was enhanced in tumor cells with H-RAS Val12-dependent activation of ERK1/2, but not in cells with H-RAS Val12-dependent activation of either the PI3K or ral guanine nucleotide dissociation stimulator signaling pathways (Fig. 1B) (Martin et al., 2008; Ihle et al., 2009). In long-term colony formation assays, sorafenib and vorinostat interacted in a synergistic manner to kill HCT116 and SW480 cells, as judged by CI values of less than 1.00 (Table 1). Similar synergistic tumor cell killing/colony formation data were obtained when an unrelated clinically used HDACI, sodium valproate, was substituted for vorinostat (Table 2).

Prior studies have demonstrated in hepatoma and renal carcinoma cells that sorafenib + vorinostat toxicity was de-

TABLE 1

Sorafenib and vorinostat synergize in colony formation assays to kill colon cancer cells

Colon cancer (HCT116, SW480) cells were treated 12 h after plating as single cells (250–1500 cells/well) in sextuplicate with vehicle (DMSO), sorafenib (3.0–6.0 μM), vorinostat (250–500 nM), or with both drugs combined, as indicated at a fixed concentration ratio, to perform median dose-effect analyses for the determination of synergy. After drug exposure (48 h), the medium was changed, and cells were cultured in drug-free media for an additional 10 to 14 days. Cells were fixed and stained with crystal violet, and colonies of >50 cells/colony counted. Colony formation data were entered into the Calcusyn program, and CI values were determined. A CI value of less than 1.00 indicates synergy; a CI value of greater than 1.00 indicates antagonism.

Cell Line	Sorafenib	Vorinostat	CI
	μM	μM	
HCT116	3.0	0.250	0.46
	4.5	0.375	0.59
	6.0	0.500	0.66
SW480	3.0	0.250	0.57
	4.5	0.375	0.59
	6.0	0.500	0.49

TABLE 2

Sorafenib and sodium valproate synergize in colony formation assays to kill colon cancer cells

Colon cancer (HCT116, SW480) cells were treated 12 h after plating as single cells (250–1500 cells/well) in sextuplicate with vehicle (DMSO), sorafenib (2.0–9.0 μM), or sodium valproate (0.33–1.5 mM), or with both drugs combined, as indicated at a fixed concentration ratio to perform median dose effect analyses for the determination of synergy. After drug exposure (48 h), the medium was changed and cells cultured in drug-free media for an additional 10 to 14 days. Cells were fixed and stained with crystal violet, and colonies of >50 cells/colony were counted. Colony formation data were entered into the Calcusyn program, and CI values were determined. A CI value of less than 1.00 indicates synergy; a CI value of greater than 1.00 indicates antagonism.

Cell Line	Sorafenib	Valproate	CI
	μM	mM	
HCT116	3.0	0.50	0.65
	4.5	0.75	0.66
	6.0	1.00	0.64
	7.5	1.25	0.49
	9.0	1.50	0.48
SW480	2.0	0.33	0.57
	3.0	0.50	0.68
	4.0	0.66	0.74

Fig. 2. Sorafenib and vorinostat toxicity is enhanced by GX15-070 in SW480 cells. A, HCT116 cells were, as indicated, infected with recombinant adenoviruses, and 24 h after infection, cells were treated with vehicle, sorafenib, vorinostat, or both drugs together. Forty-eight hours after exposure, cells were isolated and stained with Annexin V-propidium iodide, and cell viability was determined by flow cytometry (± S.E.M., $n = 3$). *, $p < 0.05$ less than corresponding value in CMV vector cells. Inset, expression of BCL-XL 24 h after infection. B, HCT116 cells were treated with vehicle or GX15-070 followed by, as indicated, vehicle, sorafenib, sodium valproate, or sorafenib + valproate. Twenty-four and 48 h after exposure, cells were isolated and viability determined via Annexin V-propidium iodide, and cell viability was determined by flow cytometry (± S.E.M., $n = 3$ independent studies). #, $p < 0.05$ greater than corresponding value in HCT116 cells (compare Fig. 1B). C, SW480 cells, 24 h after plating in triplicate, were treated with vehicle or GX15-070 followed by, as indicated, vehicle (DMSO), sorafenib, sodium valproate, or sorafenib + valproate. Twenty-four and 48 h after exposure, cells were isolated and viability determined via Annexin V-propidium iodide, and cell viability was determined by flow cytometry (± S.E.M., $n = 3$ independent studies). D, SW480 cells were transfected with siRNA molecules to knock down CD95. Twenty-four hours after transfection, cells were treated with vehicle or GX15-070 followed by, as indicated, vehicle, sorafenib, sodium valproate, or sorafenib + valproate. Twenty-four and 48 h after exposure, cells were isolated, and viability was determined via Annexin V-propidium iodide, and cell viability was determined by flow cytometry (± S.E.M., $n = 2$ independent studies). *, $p < 0.05$ less than corresponding value in siSCR transfected cells. E and F, OVCAR, SKOVIII, Rh30, and Rh41 cells were treated with vehicle or GX15-070 followed by, as indicated, vehicle, sorafenib, vorinostat, sodium valproate, sorafenib + valproate, or sorafenib + vorinostat. Forty-eight hours after exposure, cells were isolated and viability was determined via trypan blue exclusion assay (± S.E.M., $n = 3$ independent studies). #, $p < 0.05$ greater than sorafenib + vorinostat value. G and H, OVCAR and Rh41 cells were transfected with siRNA molecules to knock down CD95. Twenty-four hours after transfection, cells were treated with vehicle or GX15-070 followed by, as indicated, vehicle, sorafenib, sodium valproate, or sorafenib + valproate. Twenty-four and 48 h after exposure, cells were isolated and viability was determined via trypan blue exclusion assay (± S.E.M., $n = 2$ independent studies). *, $p < 0.05$ less than corresponding value in siSCR-transfected cells.

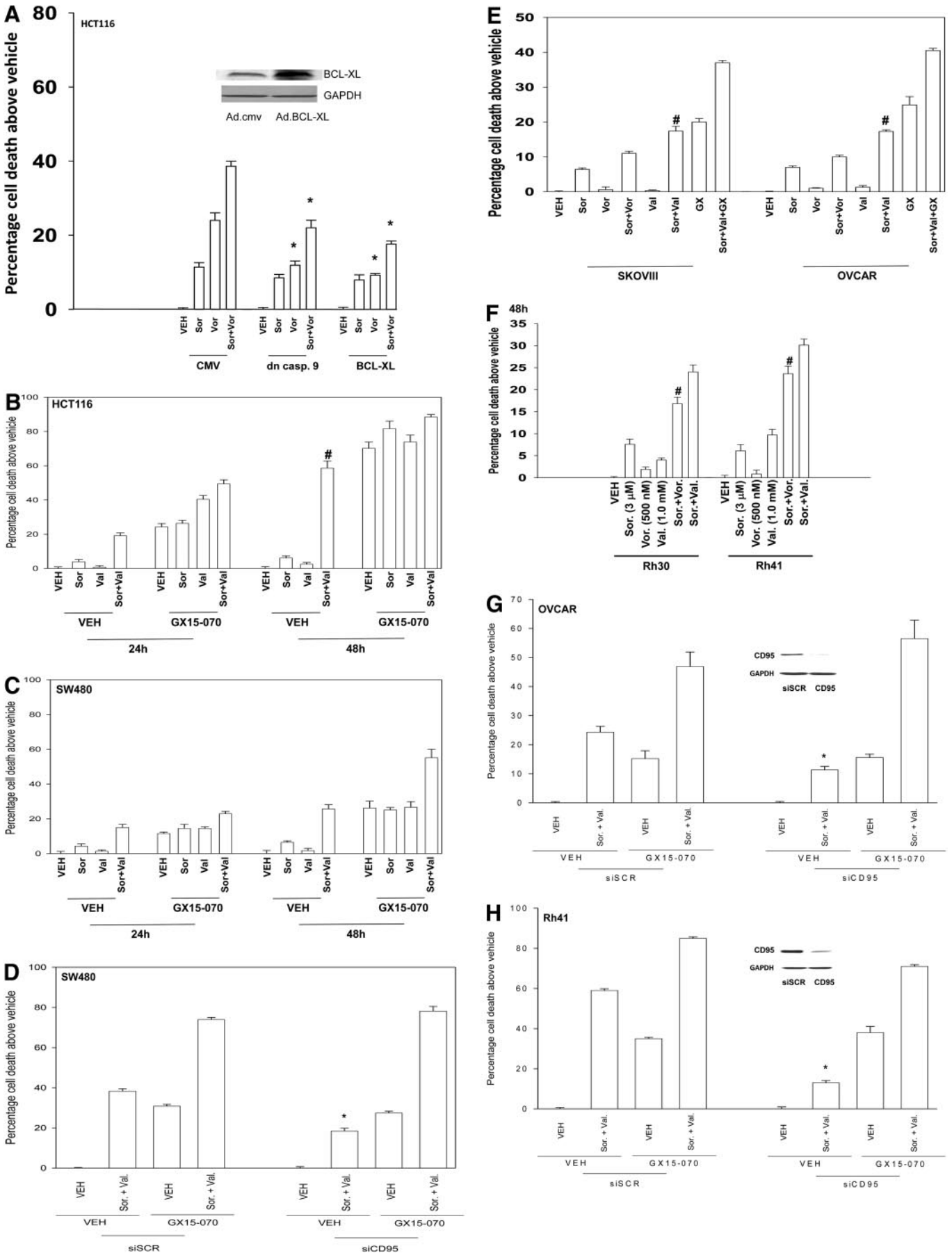

Fig. 2.

pendent on activation of CD95 (Park et al., 2008a; Zhang et al., 2008). In these studies, we also discovered that, in addition to well recognized components of the CD95-DISC (e.g., pro-caspase 8, c-FLIP-s), we also observed increased association of autophagy and ER stress regulatory proteins (e.g., ATG5, Grp78/BiP). Hence, we examined the roles of CD95 and c-FLIP-s in modulating sorafenib + vorinostat toxicity in both HCT116 and in SW480 cells. Knockdown of CD95 *increased* vorinostat and sorafenib + vorinostat toxicity in HCT116 cells, and overexpression of c-FLIP-s weakly blunted drug-induced cell killing (Fig. 1C). Knockdown of CD95 or overexpression of c-FLIP-s blocked sorafenib + vorinostat toxicity in SW480 cells (Fig. 1D). The data obtained in SW480 cells is very similar to that previously noted in liver, pancreatic, and kidney cancer cells. In HCT116 cells, sorafenib + vorinostat exposure caused the association of pro-caspase 8 and the chaperone Grp78/BiP with CD95 but did not increase plasma membrane staining for CD95 (Fig. 1E). In HCT116 cells, the amount of c-FLIP-s associated with pro-caspase 8 in the DISC was weakly increased after drug exposure. In SW480 cells, but not matched SW620 cells, sorafenib + vorinostat exposure profoundly increased CD95 plasma membrane staining; drug treatment in SW480 cells caused the association of pro-caspase 8 and Grp78/BiP with CD95 and with reduced expression of c-FLIP-s in the DISC (Fig. 1F) (Kubens and Zänker, 1998).

Overexpression of BCL-XL or expression of dominant-negative caspase 9 suppressed sorafenib + vorinostat toxicity in HCT116 cells, which supports the contention that in this cell line, the drugs were using the intrinsic pathway to kill (Fig. 2A). Because mitochondrial dysfunction was playing a role in sorafenib + vorinostat lethality in HCT116 cells, we then determined whether inhibition of protective BCL-2 family members facilitated drug-induced cell killing. Treatment of cells with pharmacologically achievable concentrations of the BCL-2/BCL-XL/MCL-1 inhibitor GX15-070 (obatoclax) significantly increased HCT116 or SW480 cell mortality (Fig. 2, B and C) (Nguyen et al., 2007). GX15-070 as a single agent was more toxic in HCT116 cells than in SW480 cells, but in HCT116 cells, GX15-070 did not strongly enhance the toxicity of sorafenib + valproate exposure. In SW480 cells, however, GX15-070 increased short-term sorafenib + valproate lethality in at least an additive fashion. A similar effect was observed in SW480 cells using long-term colony formation assays (data not shown). It is particular noteworthy that the toxic interaction in HCT116 cells between sorafenib and the class I HDACI sodium valproate was greater than the interaction between sorafenib and the pan-HDACI vorinostat. Valproic acid has been shown to affect HDAC2 levels by inducing its proteasomal degradation; whether altered HDAC2 function represents the reason for this observation will require future study (Krämer et al., 2003).

Loss of CD95 expression is common in tumors from patients with metastatic/advanced colon cancer; therefore, we next determined whether GX15-070 could facilitate sorafenib + valproate lethality in SW480 cells with reduced CD95 function. Knockdown of CD95 significantly reduced sorafenib + valproate-induced killing in SW480 cells (Fig. 2D). In CD95 knockdown cells treated with GX15-070, however, no significant reduction in sorafenib + valproate + GX15-070 lethality was observed, compared with scrambled siRNA control transfected cells. We then determined whether GX15-070 also enhanced the toxicity of sorafenib + HDACI treatment in other tumor cell types. GX15-070 increased sorafenib + valproate lethality in at least an additive fashion in short-term assays in adult human ovarian cancer cells and in human pediatric rhabdomyosarcoma cells (Fig. 2, E and F). As was observed in HCT116 cells, sodium valproate enhanced sorafenib toxicity in these cell types to a greater extent than did vorinostat. Knockdown of CD95 suppressed sorafenib + HDACI toxicity in ovarian cancer and in rhabdomyosarcoma cells, an effect that was circumvented by GX15-070 (Fig. 2, G and H). Sorafenib + HDACIs synergized to kill rhabdomyosarcoma cells in colony formation assays (Table 3). Collectively, the data in Fig. 2 demonstrate, in

TABLE 3

Sorafenib and sodium valproate synergize in colony formation assays to kill rhabdomyosarcoma cells

Rhabdomyosarcoma (Rh41) cells were treated 12 h after plating as single cells (250–1500 cells/well) in sextuplicate with vehicle (DMSO), sorafenib (2.0–9.0 μM), sodium valproate (0.33–1.5 mM), or with both drugs combined, as indicated at a fixed concentration ratio to perform median dose-effect analyses for the determination of synergy. After drug exposure (48 h), the medium was changed and cells cultured in drug-free media for an additional 10 to 14 days. Cells were fixed and stained with crystal violet, and colonies of >50 cells/colony counted. Colony formation data were entered into the Calcusyn program, and combination index (CI) values were determined. A CI value of less than 1.00 indicates synergy; a CI value of greater than 1.00 indicates antagonism.

Cell Line	Sorafenib	Valproate	CI
	μM	mM	
Rh41	3.0	0.50	0.82
	4.5	0.75	0.73
	6.0	1.00	0.40
	7.5	1.25	0.31
	9.0	1.50	0.12

Fig. 3. Expression of ceramide synthase 6 (LASS6) modulates the toxicity of sorafenib and vorinostat in SW480/SW620 colon cancer cells. A, SW480 cells in eight-well chamber slides were transfected with siRNA molecules to knock down expression of ASMase or were transfected with scrambled siRNA molecules. Twenty-four hours after transfection, cells were treated with vehicle or myriocin (1 μM), and after 30 min, cells were then exposed to vehicle or to sorafenib + vorinostat. Cells were fixed 6 h after exposure, and the amount of plasma membrane associated CD95 was determined by immunohistochemistry (± S.E.M., $n = 2$). Bottom inset, HEPG2, PANC1, OVCAR, and SW480 cells, 24 h, were transfected with siRNA molecules to knockdown expression of LASS6 or transfected with scrambled siRNA molecules; or SW480 cells were transfected with siRNA molecules to knockdown expression of ASMase. Twenty-four hours after transfection, cells were isolated and LASS6/ASMase expression was determined. B, HEPG2, PANC1, OVCAR, and SW480 cells, 24 h after plating in eight-well chamber slides were transfected with siRNA molecules to knock down expression of LASS6, or transfected with scrambled siRNA molecules. Twenty-four hours after transfection, cells were treated with vehicle or to sorafenib + valproate or sorafenib + vorinostat. Cells were fixed 6 h after exposure, and the amount of plasma membrane-associated CD95 was determined by immunohistochemistry (± S.E.M., $n = 2$). C, SW480 cells were transfected with siRNA to reduce ASMase protein levels as in A. Twenty-four hours after transfection, cells were treated with vehicle or myriocin (1 μM); after 30 min, cells were exposed to vehicle, sorafenib, vorinostat, or both drugs combined. Forty-eight and 96 h after exposure, cells were isolated and stained with trypan blue dye, and cell viability was determined by visible light microscopy (± S.E.M., $n = 2$). *, $p < 0.05$ less than corresponding value in siSCR cells; **, $p < 0.05$ less than corresponding value in siASMase cells. D, SW620 cells stably transfected with either vector control plasmid of a plasmid to express LASS6, 24 h after plating, were exposed to vehicle, sorafenib, vorinostat, or both drugs combined. Forty-eight hours after exposure, cells were isolated and stained with trypan blue dye and cell viability determined by visible light microscopy (± S.E.M., $n = 2$). #, $p < 0.05$ greater than corresponding value in empty vector cells. Inset, SW620 cells 24 h after plating in eight-well chamber slides as above, and exposed to vehicle, sorafenib, vorinostat, or both drugs combined. Cells were fixed 6 h after exposure and the amount of plasma membrane associated CD95 determined by immunohistochemistry (± S.E.M., $n = 2$).

MOL PHARM
MOLECULAR PHARMACOLOGY
aspet

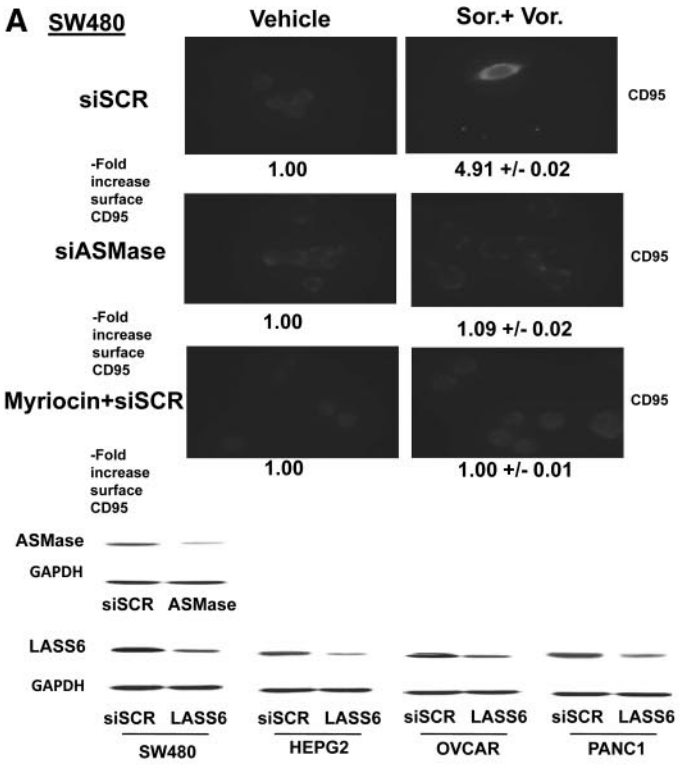

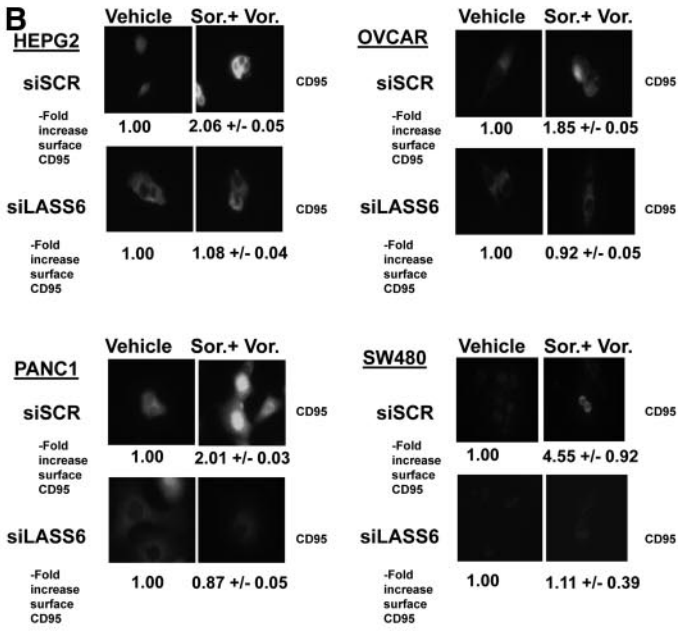

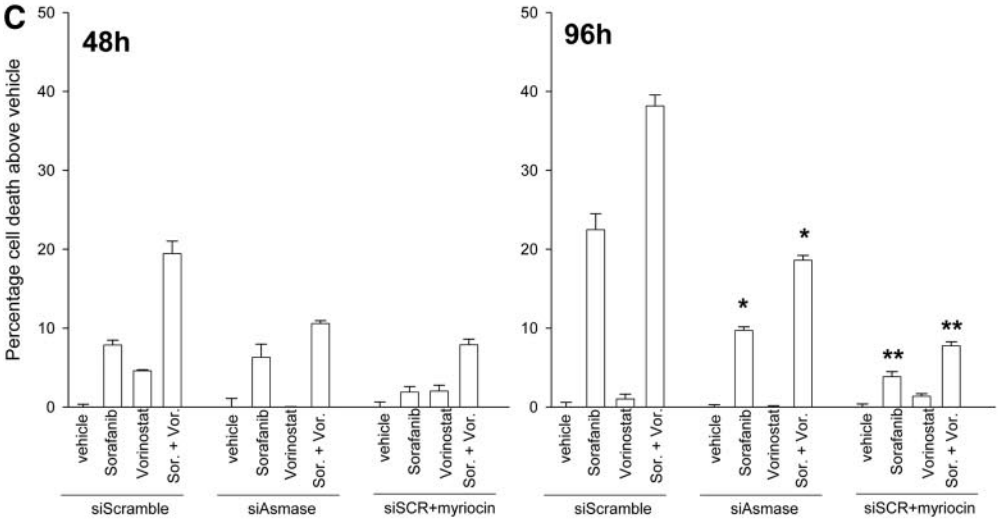

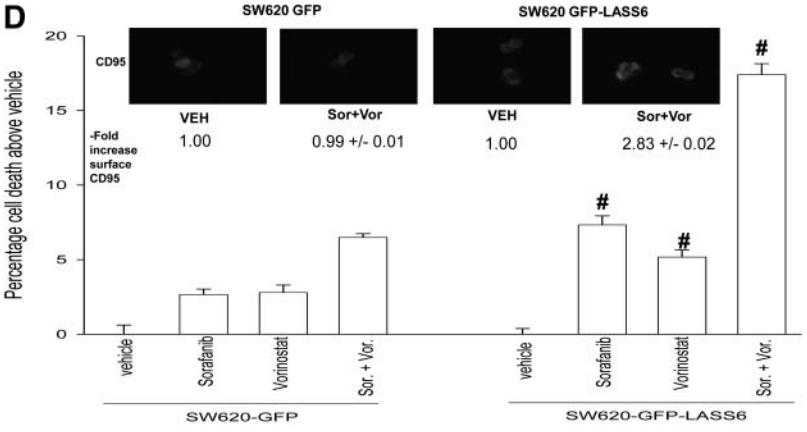

Fig. 3.

multiple types of tumor cells, that an agent that inhibits protective BCL-2 protein function enhances sorafenib + HDACI lethality.

In our prior studies using hepatoma cells, we noted that CD95 activation was inhibited by small molecule inhibitors of the de novo ceramide synthesis pathway, as well as by knockdown or knockout of acidic sphingomyelinase (ASMase). As noted previously, compared with patient-matched SW480 cells, SW620 cells were refractory to drug-induced toxicity, which correlated with a lack of CD95 activation (Fig. 1D). It has recently been shown that SW620 cells are refractory to death receptor signaling induced by tumor necrosis factor-related apoptosis-inducing ligand, which was linked to low expression of ceramide synthase 6 (LASS6), an enzyme in the de novo ceramide synthesis pathway, and with a lack of ceramide generation after tumor necrosis factor-related apoptosis-inducing ligand exposure (White-Gilbertson et al., 2009). Knockdown of ASMase expression or treatment with the de novo pathway inhibitor myriocin blocked sorafenib + vorinostat-induced CD95 activation in SW480 cells (Fig. 3A). Knockdown of LASS6 expression in SW480 cells also reduced drug-induced CD95 activation and drug-induced cell killing (Fig. 3B, data not shown). Similar data with respect to reduced CD95 activation when LASS 6 was knocked down were also observed in liver, pancreatic, and ovarian cells (Fig. 3B). Knockdown of ASMase expression or treatment with the de novo pathway inhibitor myriocin blocked sorafenib + vorinostat-induced cell killing in SW480 cells (Fig. 3C). Based on the data in Fig. 3A, we determined whether expression of LASS6 in SW620 cells facilitated drug-induced CD95 activation and cell death. Overexpression of LASS6 in SW620 cells enhanced the toxicity of sorafenib, vorinostat, and sorafenib + vorinostat, which correlated with increased activation of CD95 (Fig. 3D). Collectively, these data support the idea that expression of enzymes within the de novo ceramide pathway, particularly LASS6, is essential for CD95 activation and for the toxic actions of sorafenib and vorinostat in SW480/SW620 colon cancer cells.

We next performed studies to understand how knockdown of CD95 *enhanced* sorafenib + vorinostat toxicity in HCT116 cells. In hepatoma cells, we have previously noted that sorafenib + vorinostat exposure promoted a protective form of autophagy in a CD95- and PERK-/eIF2α-dependent fashion. In HCT116 colon cancer cells, sorafenib + vorinostat exposure promoted increased phosphorylation of PERK and the processing of LC3 (ATG8), which are suggestive of increased levels of autophagy (Fig. 4A). Grp78/BiP is a chaperone for PERK and dissociates from PERK, permitting PERK to be activated; it is noteworthy that we previously demonstrated that Grp78/BiP became associated with CD95 after drug exposure (Fig. 1C) (Park et al., 2008a). However, despite PERK's becoming phosphorylated after drug treatment, no increase in the phosphorylation of the PERK substrate eIF2α was observed. In HCT116 cells, sorafenib + vorinostat exposure promoted vesicularization of a transfected LC3-GFP construct, indicative of increased autophagy, an effect that was blocked by expression of dominant-negative PERK and by knockdown of either ATG5 or Beclin1 (Fig. 4, B and C). Expression of dominant-negative PERK blocked drug-induced increases in PERK phosphorylation, the processing of LC3, and drug-induced activation of the JNK pathway (Fig. 4B). Knockdown of CD95 expression in HCT116 cells abolished drug-induced autophagy (Fig. 4C). We then determined whether drug-induced autophagy was a protective or a toxic signal; knockdown of Beclin1 expression enhanced both vorinostat and sorafenib + vorinostat lethality (Fig. 4D). In general agreement with prior findings in liver, pancreatic, and kidney cancer cells, knockdown of Beclin1 in SW480 cells also abolished drug-induced autophagy and enhanced sorafenib + vorinostat toxicity (data not shown). Collectively, the data in Fig. 4, together with those presented in Fig. 1, demonstrate that sorafenib + vorinostat treatment promote a form of CD95 activation in HCT116 cells that is nonproductive with respect to proapoptotic signaling but is competent to stimulate an autophagic response that is cytoprotective.

We next determined whether drug-induced PERK signaling through the JNK pathway was regulated by CD95 and whether JNK pathway signaling also played a role in the regulation of autophagy. Sorafenib + vorinostat treatment activated the JNK pathway but not the p38 MAPK pathway (Fig. 5A, top blots). Inhibition of the JNK pathway enhanced the toxicity of sorafenib + vorinostat treatment (Fig. 5A, bottom graph). Knockdown of CD95 expression blocked JNK pathway activation; however, unlike prior data in hepatoma cells, knockdown of CD95 did not alter PERK activation (Fig. 5B, top blots). Thus, JNK1/2 activation requires separate drug-induced signals emanating from both CD95 and PERK.

We then examined whether JNK pathway signaling played any regulatory role in autophagy induction. Molecular inhibition of JNK1/2 signaling blocked drug-induced vesicularization of LC3-GFP (Fig. 5B, bottom graph). The autophagy regulatory protein Beclin1 has been shown to bind to BCL-2, and phosphorylation of BCL-2 by JNK1 has been proposed to cause Beclin1 to dissociate from BCL-2, thereby promoting a protective form of autophagy (Wei et al., 2008). In HCT116 cells, Beclin1 coimmunoprecipitated with BCL-2 and coprecipitation of the Beclin1 with BCL-2 was almost abolished in cells treated with sorafenib and sodium valproate (Fig. 5C). The association of Beclin1 with BCL-2 was maintained by inhibition of JNK pathway signaling, which correlated with inhibition of autophagy (Fig. 5, B and C).

Sorafenib was developed as an inhibitor of Raf kinases; however, it is now known to inhibit class III receptor tyrosine kinases. In HCT116 cells, sorafenib + vorinostat exposure did not alter AKT (Ser473) phosphorylation (Fig. 6A). As with the findings in hepatoma cells, sorafenib + vorinostat exposure transiently inhibited ERK1/2 activity 48 h after exposure. Based on these data, we used molecular approaches to define the role of each pathway in the survival response of drug treated HCT116 cells. Transient expression of dominant-negative MEK1, but not dominant-negative AKT, enhanced the toxicity of sorafenib, vorinostat, and sorafenib + vorinostat (Fig. 6A). In general, agreement with our data in Fig. 6A transient expression of activated MEK1 EE but not expression of activated AKT, suppressed sorafenib + vorinostat toxicity in HCT116 cells (Fig. 6B). Thus, the ERK1/2 pathway plays a greater regulatory role than the AKT pathway in HCT116 cells.

Discussion

The present studies were designed to examine whether sorafenib and HDACIs interact in a synergistic manner to cause cell death in colon cancer cells. In short-term cell viability as-

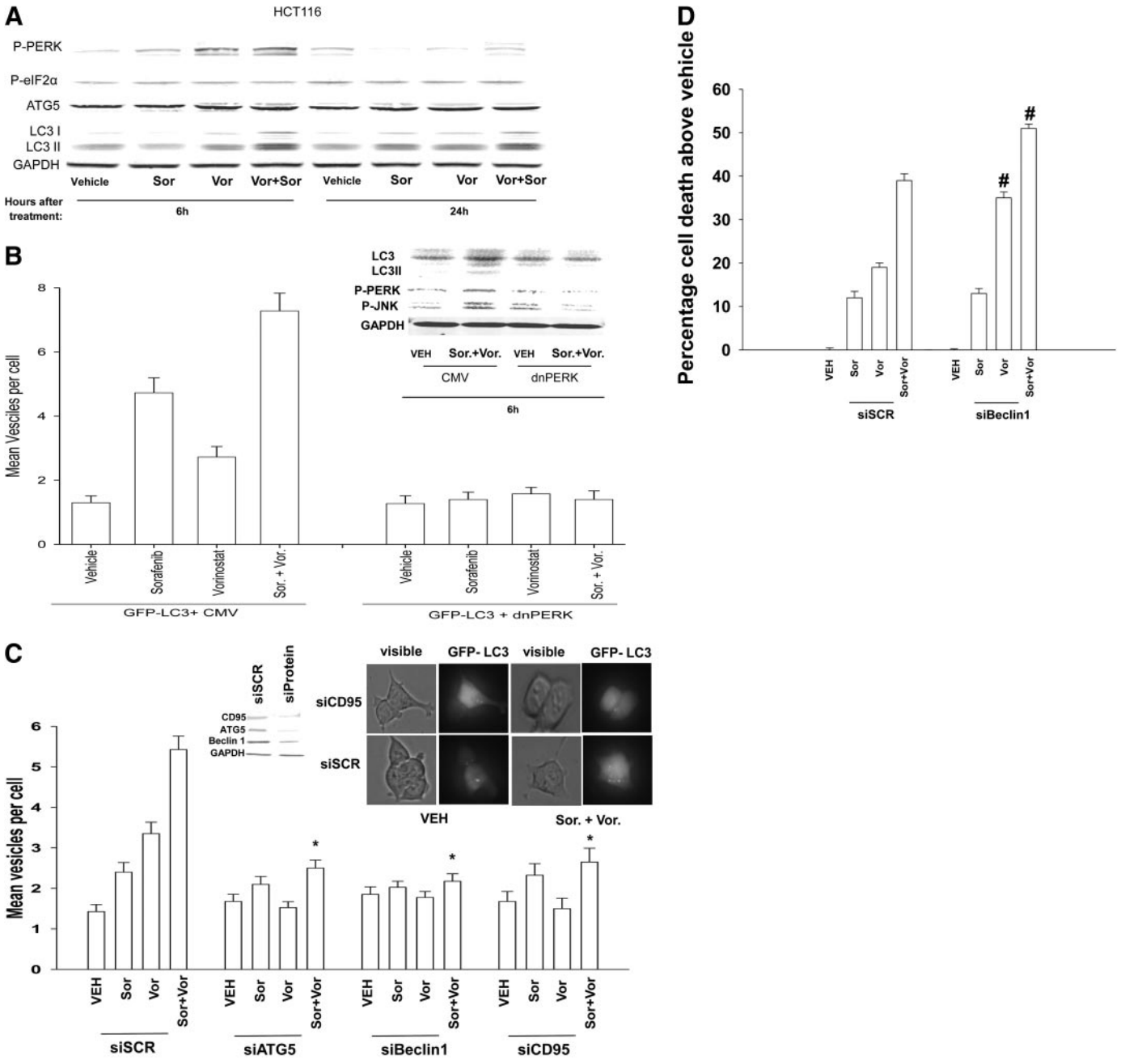

Fig. 4. Sorafenib and vorinostat interact to cause a CD95-dependent induction of autophagy in HCT116 cells that is cytoprotective. A, HCT116 cells were treated with vehicle, sorafenib, vorinostat, or both drugs combined. Cells were isolated 6 and 24 h after drug treatment and lysates subjected to SDS-PAGE and immunoblotting against the proteins indicated in the figure panel. Data are from a representative of three independent studies. B, HCT116 cells in eight-well chamber slides were transfected with a vector control plasmid (CMV) or a plasmid to express dominant-negative PERK and all cells transfected with a plasmid to express LC3-GFP. Twenty-four hours after infection, cells were treated with vehicle, sorafenib, vorinostat, or both drugs combined. Six hours after drug exposure, cells were visualized at 40× using a fluorescent microscope (Axiovert 200; Zeiss, Thornwood, NY) under fluorescent light using the FITC filter. The mean number of autophagic vesicles per cell from random fields of 40 cells was counted (± S.E.M., $n = 3$). Inset, cells transfected with vector control (CMV) or a plasmid to express dominant-negative PERK (but not LC3-GFP) were isolated 6 h after drug exposure, and lysates were subjected to SDS-PAGE and immunoblotting to determine LC3 expression and processing, PERK phosphorylation, and JNK1/2 phosphorylation (a representative $n = 3$). C, HCT116 cells in eight-well chambered glass slides were transfected with siRNA molecules to knock down expression of CD95, ATG5, or Beclin1. In parallel, cells were cotransfected with a plasmid to express LC3-GFP. Twenty-four hours after transfection, cells were treated with vehicle, sorafenib, vorinostat, or both drugs combined. Six hours after drug exposure, cells were visualized at 40× using an Axiovert 200 fluorescent microscope under fluorescent light using the FITC filter. The mean number of autophagic vesicles per cell from random fields of 40 cells was counted (± S.E.M., $n = 3$). *, $p < 0.05$ less than corresponding value in siSCR transfected cells. Inset photomicrograph, representative images taken from each of the treatment conditions in CD95 studies. Inset blot, siRNA treatment knockdown of Beclin1 or ATG5 in HCT116 cells 24 h after transfection. D, HCT116 cells in eight-well chambered glass slides were transfected with siRNA molecules to knockdown expression of Beclin1. Twenty-four hours after transfection, cells were treated with vehicle, sorafenib, vorinostat, or both drugs combined. Forty-eight hours after exposure, cells were isolated and viability was determined via trypan blue exclusion assay (± S.E.M., $n = 3$ independent studies). #, $p < 0.05$ greater than corresponding value in siSCR transfected cells.

says, sorafenib and vorinostat caused an additive to greater than additive increase in colon cancer cell death. In cells in which short-term lethality for the combination was greater than additive, a strong activation of CD95 was observed. In long-term colony formation assays, regardless of short-term CD95 activation, sorafenib and vorinostat treatment synergized to kill colon cancer cells with CI values of less than 0.70. Collectively, our findings in colon cancer cells with respect to the toxicity of sorafenib and HDACI treatment are in general agreement with those in NSCLC, renal, liver, melanoma, and pancreatic cancer cells (Park et al., 2008; Zhang et al., 2008).

In agreement with the concept that reduced basal activity in the MEK1/2 and/or PI3K pathways will reduce cellular tumorigenicity and diminish the toxicity of drugs targeting protein and lipid kinases, we found that the lethality of sorafenib, vorinostat, or sorafenib + vorinostat was sup-

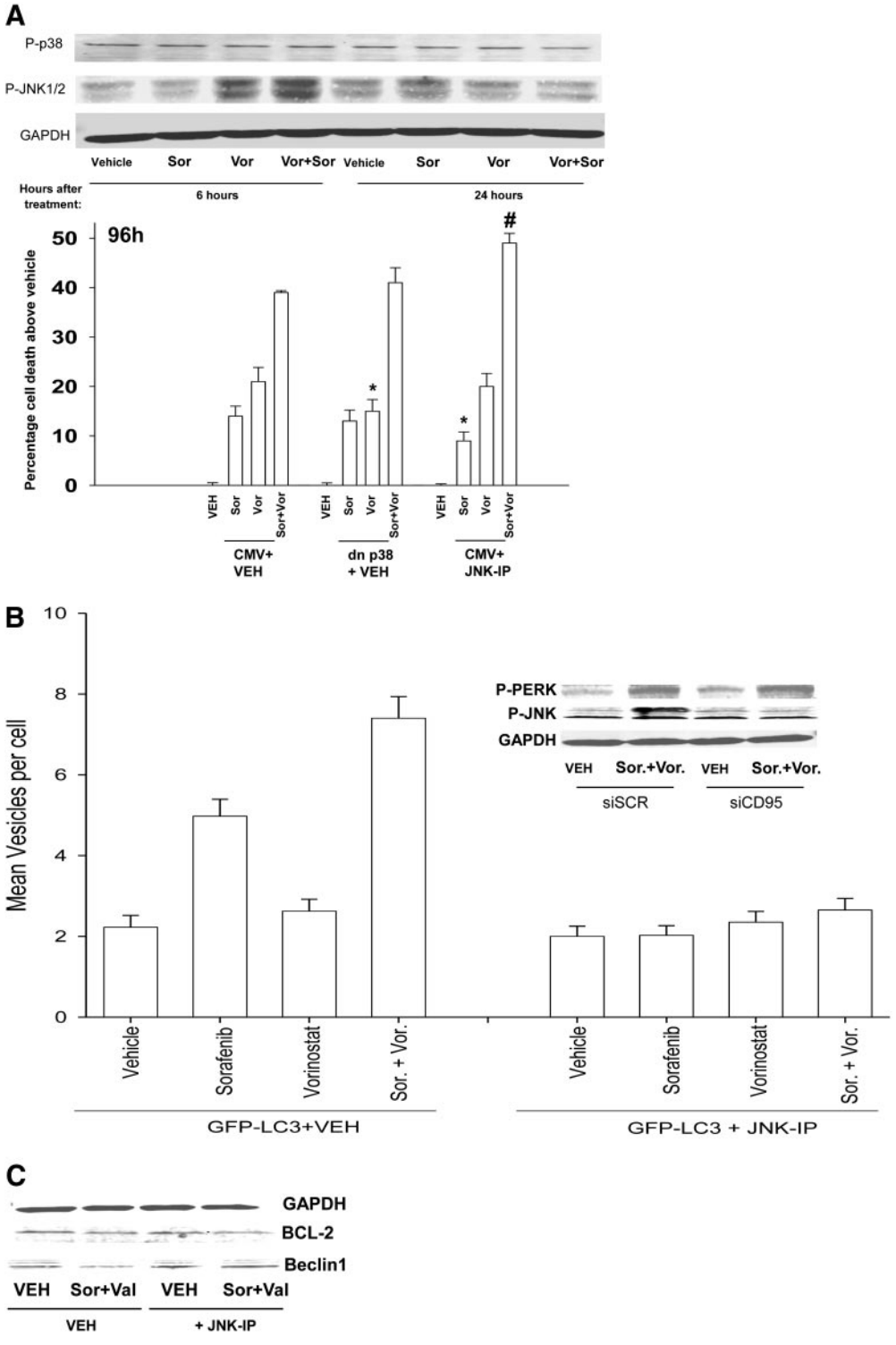

Fig. 5. Sorafenib and vorinostat toxicity in HCT116 cells is enhanced by inhibition of the JNK1/2 pathway. A, top blot, HCT116 cells were treated with either vehicle or with sorafenib and vorinostat. Six to 24 h after drug exposure, cells were isolated and subjected to SDS-PAGE and immunoblotting to determine the phosphorylation of p38 MAPK and JNK1/2. Data are from a representative of three independent studies. Bottom graph, HCT116 cells were, as indicated, infected with recombinant adenoviruses. Thirty minutes before drug exposure, cells were treated as indicated with vehicle (DMSO) or the JNK inhibitory peptide (JNK-IP, 10 μM). Twenty-four hours after infection, cells were treated with vehicle, sorafenib, vorinostat, or both drugs together. Ninety-six hours after exposure, cells were isolated and stained with Annexin V-propidium iodide and cell viability was determined by flow cytometry ($\pm$ S.E.M., $n = 3$) *, $p < 0.05$ less than corresponding value in CMV vector cells; #, $p < 0.05$ greater than corresponding value in CMV vector cells. B, top blot, HCT116 cells 24 h after plating were transfected with an siSCR or an siRNA to knock down CD95 expression. Twenty-four hours after infection, cells were treated with vehicle or with sorafenib and vorinostat. Six hours after drug exposure, cells were isolated and lysates were subjected to SDS-PAGE and immunoblotting to determine the phosphorylation status of PERK and of JNK1/2. Data are from a representative of two to three independent studies. Bottom graph, HCT116 cells in eight-well chamber slides were transfected with a plasmid to express LC3-GFP. Thirty minutes before drug exposure, cells were treated as indicated with vehicle or the JNK inhibitory peptide (JNK-IP, 10 μM). Twenty-four hours after infection, cells were treated with vehicle, sorafenib, vorinostat, or both drugs combined. Six hours after drug exposure, cells were visualized at 40$\times$ using an Axiovert 200 fluorescent microscope under fluorescent light using the FITC filter. The mean number of autophagic vesicles per cell from random fields of 40 cells was counted ($\pm$ S.E.M., $n = 3$). C, HCT116 cells were treated with vehicle or JNK inhibitory peptide (10 μM). Cells were then treated with vehicle or with sorafenib and sodium valproate. Cells were isolated 6 h after exposure, and BCL-2 was immunoprecipitated from cell lysates. Immunoprecipitates were subjected to SDS-PAGE and blotting to determine association of Beclin1 and BCL-2 in the samples ($n = 2$).

pressed by deletion of K-RAS Asp13 from HCT116 cells. This noteworthy because HCT116 cells lacking K-RAS Asp13 expression are considered only semitransformed and do not form colonies in soft agar or tumors in animals. We then investigated the relative importance of three of the best defined pathways downstream of RAS proteins that were likely to be involved in controlling drug toxicity: Raf-MEK1/2 (H-RAS Val12 Ser35); PI3K-AKT (H-RAS Val12 Cys40); RAL GDS (H-RAS Val12 Gly37). We have recently published using these cells in vitro and in vivo that activation of RAS predicted resistance to PI3K inhibitors even in the presence of activating PI3K mutations or loss of PTEN, whereas H-RAS Val12 (Cys40)-induced single activation of PI3K predicted for sensitivity to PI3K inhibitors (Ihle et al., 2009). Expression of H-RAS V12 but not point effector mutants of H-RAS Val12 that activate PI3K-AKT (Cys40) or RAL GDS (Gly37) restored the toxicity of sorafenib or vorinostat, and the drug combination, to near those levels observed in wild-type cells. In contrast to data with other effector point mutants, expression of the mutant H-RAS that elevates Raf-MEK1/2 signaling enhanced both vorinostat and sorafenib + vorinostat lethality above those in parental cells or cells expressing wild-type H-RAS V12. However, we also found in wild-type HCT116 cells that *transient* expression of dominant-negative MEK1 enhanced the toxicity of sorafenib, vorinostat, and sorafenib + vorinostat. *Transient* expression of activated MEK1 also suppressed the toxicity of sorafenib, vorinostat, and sorafenib + vorinostat. HDACI lethality can be enhanced when ERK1/2 pathway signaling is inhibited using potent small-molecule MEK1/2 inhibitors (Yu et al., 2005; Ozaki et al., 2006). Sorafenib toxicity can also be enhanced by small-molecule MEK1/2 inhibitors (S. Grant, unpublished observation). Collectively, our data in HCT116 cells lead us to conclude that although transient inhibition of ERK1/2 signaling can promote the toxicity vorinostat and facilitate sorafenib + vorinostat killing, sustained elevated basal levels of ERK1/2 activity within colon cancer cells are also predictive for enhanced vorinostat toxicity as well as enhanced sorafenib + vorinostat toxicity.

In our prior studies combining sorafenib and vorinostat in non–small-cell lung cancer, renal, liver, melanoma and pancreatic cancer cells, cell killing was PERK- and CD95-depen-

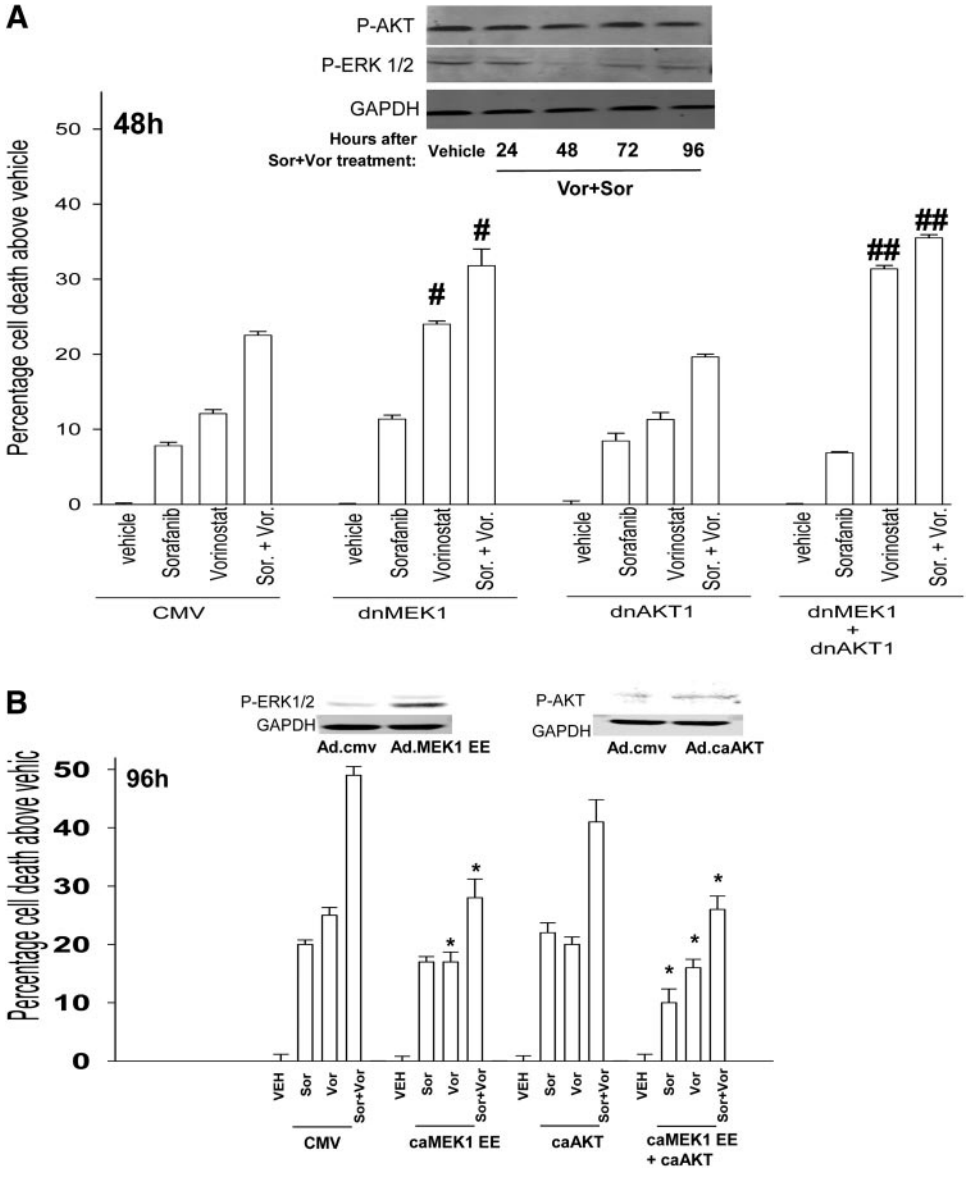

Fig. 6. Transient modulation of ERK1/2 activity, and not AKT activity, regulates sorafenib + vorinostat toxicity in HCT116 cells. A, top blot, HCT116 cells 24 h after plating were treated with either vehicle or with sorafenib + vorinostat. Twenty-four to 96 h after drug exposure, cells were isolated and subjected to SDS-PAGE and immunoblotting to determine the phosphorylation of ERK1/2 and AKT (S473). Data are from a representative of three independent studies. Bottom graph, HCT116 cells 24 h after plating were, as indicated, infected with recombinant adenoviruses. Twenty-four hours after infection, cells were treated with vehicle, sorafenib, vorinostat, or both drugs together. Forty-eight hours after exposure, cells were isolated and stained with Annexin V-propidium iodide and cell viability determined by flow cytometry (± S.E.M., $n = 3$). #, $p < 0.05$ greater than corresponding value in CMV vector cells; ##, $p < 0.05$ greater than corresponding value in dnMEK1 cells. B, HCT116 cells were, as indicated, infected with recombinant adenoviruses. Twenty-four hours after infection, cells were treated with vehicle, sorafenib, vorinostat, or both drugs together. Ninety-six hours after exposure, cells were isolated and stained with Annexin V-propidium iodide, and cell viability was determined by flow cytometry (± S.E.M., $n = 3$). *, $p < 0.05$ less than corresponding value in CMV vector cells. Inset blots: the phosphorylation of ERK1/2 and AKT (Ser473) were measured in cells expressing MEK1EE and activated AKT, respectively, 24 h after virus infection.

dent, and the induction of protective autophagy was also PERK- and CD95-dependent. We noted in SW480, OVCAR, and Rh41 cells that a similar mechanism of drug action via CD95 was extant. In HCT116 cells, however, although PERK was activated in a CD95-dependent fashion, eIF2α phosphorylation did not increase. Drug-induced eIF2α phosphorylation was previously noted to be essential for translational repression of c-FLIP-s and MCL-1 levels and in HCT116 cells, the levels of neither c-FLIP-s nor MCL-1 were suppressed after drug treatment, and the levels of c-FLIP-s remained elevated in the CD95-DISC (Park et al., 2008a). These data may explain why CD95-caspase 8 signaling was nonproductive in HCT116 cells. To our surprise, we found that knockdown of CD95 expression in HCT116 cells increased cell killing. However, we noted that drug exposure promoted a protective form of autophagy that was CD95-dependent. These data confirm and extend our prior work and argue that in some cell types, and under certain treatment conditions, death receptor signaling promotes cell survival through increased autophagy.

It has been widely reported that the expression/function of CD95 can be reduced or lost in metastatic colon cancer. We determined that a clinically relevant small molecule antagonist of BCL-2 family proteins that is entering phase II trials (GX15-070; obatoclax) enhanced sorafenib + HDACI lethality, and in cells where knockdown of CD95 reduced sorafenib + HDACI toxicity, obatoclax was capable of reverting sorafenib + HDACI lethality to levels approaching those in vector control-transfected cells; this finding was relevant in multiple tumor cell types. Additional studies will be required to determine which BH3 domain-only proteins play a central role in the death-promoting biologic effects of obatoclax in colon cancer cells.

We have shown that bile acids can promote ligand-independent ASMase and ceramide-dependent activation of CD95 in primary hepatocytes, which generated both toxic signals (caspase 8 and JNK1 activation) and protective signals (JNK2 activation) (Qiao et al., 2002, 2003). The generation of ceramide has been shown by many groups to promote ligand-independent activation of several growth factor receptors via the localization/clustering of these receptors and other signal facilitating proteins into lipid-rich domains (Barnhart et al., 2003; Kolesnick and Fuks, 2003). In melanoma and in renal and liver cancer cells, combined but not individual exposure to sorafenib and vorinostat caused rapid activation of CD95 that did not correlate with altered expression or cleavage of FAS-L (Zhang et al., 2008).

In SW480 cells, sorafenib and vorinostat exposure activated CD95 as judged by increased plasma membrane staining for CD95 as well as increased DISC formation in an ASMase- and de novo-ceramide synthesis pathway-dependent fashion. However, in patient-matched SW620 cells that have reduced ceramide synthase 6 (LASS6) expression, activation of CD95 was not observed. Our prior analyses in sorafenib + vorinostat-treated HEPG2 cells demonstrated that inhibition of the de novo synthesis pathway suppressed generation of multiple dihydro-ceramide species, particularly the C12/C14/C16 dihydro-ceramides. The six known ceramide synthase genes (LASS) are localized in the ER, and different LASS proteins have been noted to generate ceramide forms of different chain lengths, LASS5 and LASS6 being most closely linked to the generation of C14 and C16 dihydro ceramide (Ogretmen and Hannun, 2004; Futerman and Riezman, 2005). In general agreement with the hypothesis that LASS6 is a key player in the regulation of sorafenib and vorinostat toxicity, knockdown of LASS6 in SW480 cells suppressed drug-induced CD95 activation and cell killing, whereas expression of LASS6 in SW620 cells enhanced drug-induced CD95 activation and cell killing. Similar findings were also made in ovarian, liver, and pancreatic tumor cells. Whether the expression and/or the activities of LASS proteins are regulated by a combination of vorinostat-modulated protein acetylation and sorafenib-induced changes in ROS and Ca^{2+} fluxes in the ER will need to be carefully examined in future studies.

In some cell types, the toxicity of vorinostat has been linked to activation of the JNK pathway (Yu et al., 2003; Portanova et al., 2008). In HCT116 cells, we noted that vorinostat and sorafenib + vorinostat exposure increased the phosphorylation of JNK1/2, indicative of kinase activation. However, in hepatoma and renal carcinoma cells, or in SW480 cells, at the drug concentrations used in this study, the activations of JNK1/2 were either modest or not observed (unpublished observations). Signaling by the JNK pathway has been linked to growth promoting signals as well as both pro- and antiapoptotic regulation (Hochedlinger et al., 2002; Qiao et al., 2003; Liu et al., 2004; Wang et al., 2007). Inhibition of JNK1/2 using a molecular tool modestly *enhanced* sorafenib + vorinostat toxicity in HCT116 cells; our somewhat surprising finding became more easily understood when we noted that activation of JNK1/2 was dependent on expression of CD95 and was blocked by expression of dominant-negative PERK. JNK signaling decreased the amount of Beclin1 coprecipitating with BCL-2 and in drug-treated cells lacking JNK activation, more Beclin1 remained associated with BCL-2 than under vehicle or drug treatment conditions in the absence of JNK pathway blockade. This is in agreement with the concept that JNK signaling regulates the Beclin1-BCL-2 interaction, wherein JNK signaling promotes autophagy by causing Beclin1 release from BCL-2 (Wei et al., 2008). Further analysis of the upstream molecular events that regulate JNK pathway activation by CD95 and PERK will require studies beyond the scope of the present manuscript.

In conclusion, sorafenib and vorinostat interact to kill multiple colon cancer cell types. Unlike tumor cell types previously examined, such as non–small-cell lung cancer, renal, liver, melanoma, and pancreatic cancer cells, cell killing in colon cancer cells occurs via both CD95-dependent and -independent mechanisms. In all tumor cell types examined thus far, however, the induction of mitochondrial dysfunction and activation of the intrinsic pathway play central roles in drug lethality. Further studies will be required to translate the findings of this manuscript for colon cancer into animal models and ultimately the clinic.

References

Allan LA, Morrice N, Brady S, Magee G, Pathak S, and Clarke PR (2003) Inhibition of caspase-9 through phosphorylation at Thr 125 by ERK MAPK. *Nat Cell Biol* **5:**647–654.

Bali P, Pranpat M, Swaby R, Fiskus W, Yamaguchi H, Balasis M, Rocha K, Wang HG, Richon V, and Bhalla K (2005) Activity of suberoylanilide hydroxamic Acid against human breast cancer cells with amplification of her-2. *Clin Cancer Res* **11:**6382–6389.

Barnhart BC, Alappat EC, and Peter ME (2003) The CD95 type I/type II model. *Semin Immunol* **15:**185–193.

Dasmahapatra G, Yerram N, Dai Y, Dent P, and Grant S (2007) Synergistic interactions between vorinostat and sorafenib in chronic myelogenous leukemia cells involve Mcl-1 and p21CIP1 down-regulation. *Clin Cancer Res* **13:**4280–4290.

Davies BR, Logie A, McKay JS, Martin P, Steele S, Jenkins R, Cockerill M, Cartlidge S, and Smith PD (2007) AZD6244 (ARRY-142886), a potent inhibitor of mitogen-activated protein kinase/extracellular signal-regulated kinase kinase 1/2 kinases: mechanism of action in vivo, pharmacokinetic/pharmacodynamic relationship, and potential for combination in preclinical models. *Mol Cancer Ther* **6:**2209–2219.
Dent P (2005) MAP kinase pathways in the control of hepatocyte growth, metabolism and survival, in *Signaling Pathways in Liver Diseases* (DuFour JF, Clavien PA eds) pp 223–238, Springer, New York.
Dent P, Yacoub A, Fisher PB, Hagan MP, and Grant S (2003) MAPK pathways in radiation responses. *Oncogene* **22:**5885–5896.
Flaherty KT (2007) Sorafenib: delivering a targeted drug to the right targets. *Expert Rev Anticancer Ther* **7:**617–626.
Futerman AH and Riezman H (2005) The ins and outs of sphingolipid synthesis. *Trends Cell Biol* **15:**312–318.
Gollob JA (2005) Sorafenib: scientific rationales for single-agent and combination therapy in clear-cell renal cell carcinoma. *Clin Genitourin Cancer* **4:**167–174.
Grant S and Dent P (2004) Kinase inhibitors and cytotoxic drug resistance. *Clin Cancer Res* **10:**2205–2207.
Gregory PD, Wagner K, and Hörz W (2001) Histone acetylation and chromatin remodeling. *Exp Cell Res* **265:**195–202.
Hegde SR, Sun W, and Lynch JP (2008) Systemic and targeted therapy for advanced colon cancer. *Expert Rev Gastroenterol Hepatol* **2:**135–149.
Hochedlinger K, Wagner EF, and Sabapathy K (2002) Differential effects of JNK1 and JNK2 on signal specific induction of apoptosis. *Oncogene* **21:**2441–2445.
Ihle NT, Lemos R Jr, Wipf P, Yacoub A, Mitchell C, Siwak D, Mills GB, Dent P, Kirkpatrick DL, and Powis G (2009) Mutations in the phosphatidylinositol-3-kinase pathway predict for antitumor activity of the inhibitor PX-866 whereas oncogenic Ras is a dominant predictor for resistance. *Cancer Res* **69:**143–150.
Kolesnick R and Fuks Z (2003) Radiation and ceramide-induced apoptosis. *Oncogene* **22:**5897–5906.
Krämer OH, Zhu P, Ostendorff HP, Golebiewski M, Tiefenbach J, Peters MA, Brill B, Groner B, Bach I, Heinzel T, et al. (2003) The histone deacetylase inhibitor valproic acid selectively induces proteasomal degradation of HDAC2. *EMBO J* **22:**3411–3420.
Kubens BS and Zänker KS (1998) Differences in the migration capacity of primary human colon carcinoma cells (SW480) and their lymph node metastatic derivatives (SW620). *Cancer Lett* **131:**55–64.
Kwon SH, Ahn SH, Kim YK, Bae GU, Yoon JW, Hong S, Lee HY, Lee YW, Lee HW, and Han JW (2002) Apicidin, a histone deacetylase inhibitor, induces apoptosis and Fas/Fas ligand expression in human acute promyelocytic leukemia cells. *J Biol Chem* **277:**2073–2080.
Ley R, Balmanno K, Hadfield K, Weston C, and Cook SJ (2003) Activation of the ERK1/2 signaling pathway promotes phosphorylation and proteasome-dependent degradation of the BH3-only protein, Bim. *J Biol Chem* **278:**18811–18816.
Li N, Batt D, and Warmuth M (2007) B-Raf kinase inhibitors for cancer treatment. *Curr Opin Investig Drugs* **8:**452–456.
Liu J, Minemoto Y, and Lin A (2004) c-Jun N-terminal protein kinase 1 (JNK1), but not JNK2, is essential for tumor necrosis factor alpha-induced c-Jun kinase activation and apoptosis. *Mol Cell Biol* **24:**10844–10856.
Marks PA, Miller T, and Richon VM (2003) Histone deacetylases. *Curr Opin Pharmacol* **3:**344–351.
Martin AP, Miller A, Emad L, Rahmani M, Walker T, Mitchell C, Hagan MP, Park MA, Yacoub A, Fisher PB, et al. (2008) Lapatinib resistance in HCT116 cells is mediated by elevated MCL-1 expression and decreased BAK activation and not by ERBB receptor kinase mutation. *Mol Pharmacol* **74:**807–822.
Mitchell C, Park MA, Zhang G, Han SI, Harada H, Franklin RA, Yacoub A, Li PL, Hylemon PB, Grant S, et al. (2007) 17-Allylamino-17-demethoxygeldanamycin enhances the lethality of deoxycholic acid in primary rodent hepatocytes and established cell lines. *Mol Cancer Ther* **6:**618–632.
Mori M, Uchida M, Watanabe T, Kirito K, Hatake K, Ozawa K, and Komatsu N (2003) Activation of extracellular signal-regulated kinases ERK1 and ERK2 induces Bcl-xL up-regulation via inhibition of caspase activities in erythropoietin signaling. *J Cell Physiol* **195:**290–297.
Nguyen M, Marcellus RC, Roulston A, Watson M, Serfass L, Murthy Madiraju SR, Goulet D, Viallet J, Bélec L, Billot X, et al. (2007) Small molecule obatoclax (GX15-070) antagonizes MCL-1 and overcomes MCL-1-mediated resistance to apoptosis. *Proc Natl Acad Sci U S A* **104:**19512–19517.
Ogretmen B and Hannun YA (2004) Biologically active sphingolipids in cancer pathogenesis and treatment. *Nat Rev Cancer* **4:**604–616.
Ozaki K, Minoda A, Kishikawa F, and Kohno M (2006) Blockade of the ERK pathway markedly sensitizes tumor cells to HDAC inhibitor-induced cell death. *Biochem Biophys Res Commun* **339:**1171–1177.
Pang RW and Poon RT (2007) From molecular biology to targeted therapies for hepatocellular carcinoma: the future is now. *Oncology* **72 (Suppl 1):**30–44.
Park MA, Yacoub A, Rahmani M, Zhang G, Hart L, Hagan MP, Calderwood SK, Sherman MY, Koumenis C, Spiegel S, et al. (2008b) OSU-03012 stimulates PKR-like endoplasmic reticulum-dependent increases in 70-kDa heat shock protein expression, attenuating its lethal actions in transformed cells. *Mol Pharmacol* **73:**1168–1184.
Park MA, Zhang G, Martin AP, Hamed H, Mitchell C, Hylemon PB, Graf M, Rahmani M, Ryan K, Liu X, et al. (2008a) Vorinostat and sorafenib increase ER stress, autophagy and apoptosis via ceramide-dependent CD95 and PERK activation. *Cancer Biol Ther* **7:**1648–1662.
Park MA, Zhang G, Mitchell C, Rahmani M, Hamed H, Hagan MP, Yacoub A, Curiel DT, Fisher PB, Grant S, et al. (2008c) Mitogen-activated protein kinase kinase 1/2 inhibitors and 17-allylamino-17-demethoxygeldanamycin synergize to kill human gastrointestinal tumor cells in vitro via suppression of c-FLIP-s levels and activation of CD95. *Mol Cancer Ther* **7:**2633–2648.
Parkin DM, Bray F, Ferlay J, and Pisani P (2005) Global cancer statistics, 2002. *CA Cancer J Clin* **55:**74–108.
Portanova P, Russo T, Pellerito O, Calvaruso G, Giuliano M, Vento R, and Tesoriere G (2008) The role of oxidative stress in apoptosis induced by the histone deacetylase inhibitor suberoylanilide hydroxamic acid in human colon adenocarcinoma HT-29 cells. *Int J Oncol* **33:**325–331.
Qiao L, Han SI, Fang Y, Park JS, Gupta S, Gilfor D, Amorino G, Valerie K, Sealy L, Engelhardt JF, et al. (2003) Bile acid regulation of C/EBPbeta, CREB, and c-Jun function, via the extracellular signal-regulated kinase and c-Jun NH2-terminal kinase pathways, modulates the apoptotic response of hepatocytes. *Mol Cell Biol* **23:**3052–3066.
Qiao L, Studer E, Leach K, McKinstry R, Gupta S, Decker R, Kukreja R, Valerie K, Nagarkatti P, El Deiry W, et al. (2001) Deoxycholic acid (DCA) causes ligand-independent activation of epidermal growth factor receptor (EGFR) and FAS receptor in primary hepatocytes: inhibition of EGFR/mitogen-activated protein kinase-signaling module enhances DCA-induced apoptosis. *Mol Biol Cell* **12:**2629–2645.
Qiao L, Yacoub A, Studer E, Gupta S, Pei XY, Grant S, Hylemon PB, and Dent P (2002) Inhibition of the MAPK and PI3K pathways enhances UDCA-induced apoptosis in primary rodent hepatocytes. *Hepatology* **35:**779–789.
Rahmani M, Davis EM, Bauer C, Dent P, and Grant S (2005) Apoptosis induced by the kinase inhibitor BAY 43–9006 in human leukemia cells involves down-regulation of Mcl-1 through inhibition of translation. *J Biol Chem* **280:**35217–35227.
Rahmani M, Davis EM, Crabtree TR, Habibi JR, Nguyen TK, Dent P, and Grant S (2007b) The kinase inhibitor sorafenib induces cell death through a process involving induction of endoplasmic reticulum stress. *Mol Cell Biol* **27:**5499–5513.
Rahmani M, Nguyen TK, Dent P, and Grant S (2007a) The multikinase inhibitor sorafenib induces apoptosis in highly imatinib mesylate-resistant bcr/abl + human leukemia cells in association with signal transducer and activator of transcription 5 inhibition and myeloid cell leukemia-1 down-regulation. *Mol Pharmacol* **72:**788–795.
Rini BI (2006) Sorafenib. *Expert Opin Pharmacother* **7:**453–461.
Strumberg D (2005) Preclinical and clinical development of the oral multikinase inhibitor sorafenib in cancer treatment. *Drugs Today (Barc)* **41:**773–784.
Valerie K, Yacoub A, Hagan MP, Curiel DT, Fisher PB, Grant S, and Dent P (2007) Radiation-induced cell signaling: inside-out and outside-in. *Mol Cancer Ther* **6:**789–801.
Venturelli S, Armeanu S, Pathil A, Hsieh CJ, Weiss TS, Vonthein R, Wehrmann M, Gregor M, Lauer UM, and Bitzer M (2007) Epigenetic combination therapy as a tumor-selective treatment approach for hepatocellular carcinoma. *Cancer* **109:**2132–2141.
Wang Y, Singh R, Massey AC, Kane SS, Kaushik S, Grant T, Xiang Y, Cuervo AM, and Czaja MJ (2008) Loss of macroautophagy promotes or prevents fibroblast apoptosis depending on the death stimulus. *J Biol Chem* **283:**4766–4777.
Wang YF, Jiang CC, Kiejda KA, Gillespie S, Zhang XD, and Hersey P (2007) Apoptosis induction in human melanoma cells by inhibition of MEK is caspase-independent and mediated by the Bcl-2 family members PUMA, Bim, and Mcl-1. *Clin Cancer Res* **13:**4934–4942.
Wei Y, Pattingre S, Sinha S, Bassik M, and Levine B (2008) JNK1-mediated phosphorylation of Bcl-2 regulates starvation-induced autophagy. *Mol Cell* **30:**678–688.
White-Gilbertson S, Mullen T, Senkal C, Lu P, Ogretmen B, Obeid L, and Voelkel-Johnson C (2009) Ceramide synthase 6 modulates TRAIL sensitivity and nuclear translocation of active caspase-3 in colon cancer cells. *Oncogene* **28:**1132–1141.
Wise LD, Turner KJ, and Kerr JS (2007) Assessment of developmental toxicity of vorinostat, a histone deacetylase inhibitor, in Sprague-Dawley rats and Dutch Belted rabbits. *Birth Defects Res B Dev Reprod Toxicol* **80:**57–68.
Yacoub A, Park MA, Gupta P, Rahmani M, Zhang G, Hamed H, Hanna D, Sarkar D, Lebedeva IV, Emdad L, et al. (2008) Caspase-, cathepsin-, and PERK-dependent regulation of MDA-7/IL-24-induced cell killing in primary human glioma cells. *Mol Cancer Ther* **7:**297–313.
Yu C, Dasmahapatra G, Dent P, and Grant S (2005) Synergistic interactions between MEK1/2 and histone deacetylase inhibitors in BCR/ABL + human leukemia cells. *Leukemia* **19:**1579–1589.
Yu C, Subler M, Rahmani M, Reese E, Krystal G, Conrad D, Dent P, and Grant S (2003) Induction of apoptosis in BCR/ABL + cells by histone deacetylase inhibitors involves reciprocal effects on the RAF/MEK/ERK and JNK pathways. *Cancer Biol Ther* **2:**544–551.
Zhang G, Park MA, Mitchell C, Hamed H, Rahmani M, Martin AP, Curiel DT, Yacoub A, Graf M, Lee R, et al. (2008) Vorinostat and sorafenib synergistically kill tumor cells via FLIP suppression and CD95 activation. *Clin Cancer Res* **14:**5385–5399.

Address correspondence to: Dr. Paul Dent, Department of Biochemistry and Molecular Biology, 401 College Street, Massey Cancer Center, Room 280a, Box 980035, Virginia Commonwealth University, Richmond VA 23298-0035. E-mail: pdent@vcu.edu